Weldment Fracture Toughness of an Aluminum-Copper Alloy

The effects of surface flaws, primary and repair welding, and postweld treatment on failure stress are determined for specific regions in 2021 aluminum welds

BY J. G. BJELETICH, T. M. MORTON AND R. E. LEWIS

ABSTRACT. The effects of surface flaws on the fracture strength of gas tungsten-arc weldments of the aluminum-copper alloy designated 2021 are studied. Surface-flaw fracture toughness parameters are determined for the near heat-affected and weld metal zones of the weldments in a variety of conditions, including those produced by variations in the primary welding techniques, repair welded, unaged and postweld aged. Postweld aging increases the mechanical strength of the weldments and the toughness of the weld metal by about 15%. However, these enhanced properties are accompanied by approximately a 30% sacrifice in the minimum toughness of a narrow region in the heat-affected zone immediately adjacent to the weld fusion line. The diminished toughness in this region is attributed to the presence of an intermetallic phase in the grain boundaries. In similar locations bordering deep manual repairs in aged welds, the intermetallic phase is not prevalent and the fracture toughness value is double that found adjacent to repair areas. Toughness of the aged weldments is not sensitive to minor variations in the primary welding procedures.

The test approach and analysis described are generally applicable for providing the required information to prove safe-life capability of a specific design. The specific data developed may be useful to those who are considering engineering application of 2021 aluminum alloy weldments.

J. G. BJELETICH, T. M. MORTON and R. E. LEWIS are respectively Research Scientist, Senior Scientist and Staff Scientist at Lockheed Palo Alto Research Laboratory, Palo Alto, California.

Objective

The objective of this study was to evaluate the fracture resistance of weldments of the aluminum-copper alloy, 2021, in the stress range encountered in the operation of a specific aerospace fuel storage tank. The need for the fracture toughness data was prompted by the post-fabrication, safe-life analysis of the storage vessel, originally designed with the classical factor of safety concept. The paper is intended to provide useful data to materials engineers considering the application of similar 2021 aluminum alloy weldments. It is also intended to illustrate: (1) the experimental approach employed to provide the information required in performing a safe-life analyses of an engineering structure; and, (2) the roles that weldment mechanical integrity (strength) and weldment toughness must play in the selection of a candidate material for a specific engineering application.

Background

A candidate alloy intended to provide a favorable compromise of mechanical and physical characteristics for space system tankage or pressure vessel applications is the aluminum-copper alloy of relatively recent development, 2021 (Ref. 1). Material properties of importance in these applications include the strength-to-density ratio, fracture toughness parameter and weldability. At the service temperatures and in the environments encountered by space tankage, aluminum-copper alloys are one of several alloy systems that offer the promise of a desirable combination of these prop-

erties (Ref. 2). Interest in candidate aluminum alloys such as 2021 stems from their advantage in low material costs and relative ease in fabrication.

Fabrication of space tankage of the most efficient design usually requires metal joining by welding. Even in the most carefully performed welding operations, flaws or defects in the form of surface or subsurface cracks, incomplete fusion, inadequate joint penetration, undercut, porosity, cavities or solid inclusions are not an uncommon occurrence. The detriment to the mechanical integrity of high strength weldments represented by the presence of these flaws is well known. Consequently, the mechanical and physical characteristics of the weld areas are significant contributors to the efficiency of reliable or safe-life welded tankage. As a result, the weldability of a candidate alloy becomes a prime factor in its consideration.

Weldability not only refers to a material's capability to be joined readily by various welding processes but also implies subsequent satisfactory mechanical performance of the weld. The efficient use of any candidate metal alloy requires a knowledge of the factors that govern its weldability. In pressure vessels for space applications, two of the most important of these factors are mechanical strength and flaw tolerance.

Presently, the most useful methods available for evaluating a material's tolerance to flaws are based upon the principles of elastic fracture mechanics theory. This theory has introduced the concept of a single valued parameter — critical stress intensity factor — to relate flaw size and fracture stress. This parameter, also referred to as the fracture toughness, represents the resistance to the unstable crack propagation stage of the fracture process. Although the critical stress intensity factor depends upon many variables; e.g., material thickness, weld procedures, heat treatment, etc., it can be evaluated experimentally.

Methods of determining the fracture toughness parameter in relatively thick sections — plane strain conditions — of a given specimen geometry are well established (Ref. 3). During plane strain conditions, this parameter is considered to be an inherent material characteristic and by convention is designated, K_{Ic}. However, there is a lack of reliable correlation between the behavior of the accepted specimens for plane strain fracture toughness measurements and the fracture behavior of some pressure vessels. In general, material thicknesses used in aerospace pressure vessels are too small to provide the necessary elastic constraints for plane strain conditions. Additionally, the type of flaw of greatest concern in tankage — surface flaws — is the least understood analytically.

Table 1 — Composition of 2021 Aluminum Alloy (weight percent)

Silicon	0.20 max
Iron	0.30 max
Copper	5.8 - 6.8
Manganese	0.20 - 0.40
Zinc	0.10 max
Titanium	0.02 - 0.10
Vanadium	0.05 - 0.15
Zirconium	0.05 - 0.25
Cadmium	0.05 - 0.20
Tin	0.03 - 0.08
Others	0.15 max
Aluminum	Balance

Reliable predictions of flaw behavior can be realized in many cases where valid plane strain fracture toughness solutions do not have direct applicability. In these instances, predicted performance is based upon carefully evaluated results of specimens tested under laboratory simulated service conditions or on semi-empirical relationships established from parametric studies. In either case, the presently accepted approach is to model the flaws to be found in the pressure vessel using surface-flawed specimens of the same material and thickness as the vessel.

An analytic formulation of the critical stress intensity factor developed by Irwin (Ref. 4) for a semi-elliptical surface-flawed specimen is

$$K_{Ic} = 1.1\sigma\sqrt{\pi a/Q} \qquad (1)$$

where

K_{Ic} = stress intensity factor at onset of unstable fracture, ksi-in$^{1/2}$

σ = stress on gross section, ksi

(a/Q) = normalized crack depth, in.

This expression shows the severity of a semi-elliptical flaw to be characterized by its depth, a, modified by a factor, Q. Experience has shown that the quantity, a/Q, sometimes called the normalized crack depth, correlates the effects of surface flaws very well (Ref. 5). The function, Q, depends primarily on the ratio of the flaw depth to half length, a/c, and secondarily on a correction term for the plastic deformation at the flaw front (Ref. 4).

A cogent relationship between fracture stress and flaw size can be obtained using Eq. (1). The application of the result is limited to surface flaws in material thicknesses that correspond to the specimen thickness from which the result was obtained. To differentiate it from the valid plane strain value, the critical stress intensity calculated from Eq. (1) and reported herein is designated K_{IE}.

The fuel storage pressure vessel, which was qualified for safe-life operation by the findings of this study, is a five foot diameter sphere constructed of 2021 aluminum alloy and operates in the temperature range, 70 to 120 F. It consists of two shear spun hemispheres gas tungsten-arc (GTA) welded to an equatorial Y-ring forging.

Experimental Procedures

Materials

The material used to fabricate the test specimens in this program was 2021 aluminum alloy plate, bar stock and rolled-ring forging. All of the material was supplied by the Aluminum Company of America. The chemical composition of the 2021 alloy is the same as that of aluminum alloy 2219, except 2021 has additions of small amounts of cadmium and tin (see Table 1). The plate material was received in the H210 temper (strain hardened and partially annealed, shear forming quality disks) and the bar stock and rolled-ring forging in the T315X temper (solution treated, artificially preaged and stretch-stress relieved).

Plate material for test specimens was taken from panels that had been sectioned from either 1/2 or 1 in. thick, 5 ft diam, shear-forming disks. The panels were solution treated for 3 h at 985 F and water quenched. After solution treating, the panels were machined by milling to a final thickness of 0.330 ± 0.005 in. Prior to machining, panels that exhibited distortion were mechanically straightened. Each machined panel was given an aging treatment of 10 h at 325 F before it was used to prepare weldments for evaluation.

To obtain panels of forging material, several 12 in. segments were removed from a rolled-ring forging. After an aging treatment of 10 to 12 h at a temperature between 330 to 350 F, two panels, nominally 12 by 6 in. and a thickness of 0.330 ± 0.005 in. were milled from each segment. These aged and machined to size panels were used to fabricate weldments.

The 2.5 in. thick bar stock was cut and machined to size in the same manner as the plate material and given the same heat treatment as the forged material.

Preparation of Weldments

Three types of weld panels were produced: (1) plate to plate; (2) plate to forging; and (3) plate to bar stock. Most of the weldments were joined by a direct current, straight polarity (dcsp) GTA, two pass, "suspended bead" technique* with the weld direction parallel to the principal rolling direction of the plate panels. The details of the welding procedure are given in Table 2. Unless otherwise noted, all weldments were postweld aged at 340 F for 12.5 h.

Primary welding process variations investigated included: plus and minus 10 amperes in welding current, and a third welding pass to simulate start-stop regions in tankage closure welds.

Weldments with reworked welds varying in length from 1 to 2 in. and with a repair depth of either 0.25 or 0.33 in. were also evaluated. The weld regions to be reworked were mechanically gouged out to the specified depth and then manually repaired with up to eight passes using 2319 bare filler metal.

All of the weldments used to fabricate the test specimens in this program were inspected radiographically and with dye penetrant. Detected defects within a welded panel were indicated with surface markings and excluded in subsequent test specimen fabrication.

Specimen Preparation

Specimen configuration is shown in Fig. 1. The specimen width was 2.3 to 3.0 in., the length 12 in., and the thickness nominally 0.3 in. Many of the weldment panels were warped. Those that exhibited moderate amounts of warpage and misalignment were machined directly into specimens. The thickness of these specimens was slightly less than 0.3 in. The more severely warped weldment panels were mechanically straightened before preparing test specimens to conserve specimen thickness. No effect of the straightening operation on mechanical properties was noted in subsequent tensile tests.

Starter flaws were introduced into the root side of each specimen using either an electrical discharge machine with a preshaped semi-elliptical electrode or a jeweler's circular power saw, producing a narrow slot with a depth contour approaching a semi-ellipse. Both types of starter flaws were sharpened to a root radius of about 0.0001 in. by scribing their troughs with a sharp steel blade. In most specimens, the sharpened starter flaws were extended to fatigue crack acuity by the application of constant amplitude, axial tension-tension, or bending tension-tension cyclic loads. Flaw surface length was less than one-third specimen width in all cases. A few specimens were tested without being fatigue precracked.

Preliminary tests indicated the weldment region of minimum toughness is in the near heat-affected zone. This region is located between 0.005 and 0.015 in. from the weld fusion line. Positioning the starter flaw in this region is dependent upon the cross-sectional profile of the weld zone. To place the tip of the flaw in the desired location, it was necessary to reveal the surface traces of the weld zone by etching with a dilute solution of NaOH.

With the etched traces of the weld zone as a reference, the intersection of the flaw with the near heat-affected zone was located on the specimen side edges. By geometric construction, a line connecting the two intersection locations was scribed on the specimen's root surface. Surface flaws were introduced using the constructed line and the specimen axis for positioning the preshaped electrode or jeweler's saw. A schematic representation of the test specimen with a flaw in the near heat-affected zone is shown in Fig. 1. Starter flaws in the weld zone were similarly introduced with the location along the weld centerline.

Tensile Test Procedure

Tensile property tests were conducted in 1 in. wide nonreduced section specimens. Loads were applied with a Universal testing machine whose accuracy meets or exceeds the accepted ASTM standard of 1% of indicated load. Specimens were loaded at nominal cross-head displacement rate of 0.005 in./min all the way to fracture. Strains were measured in some of the specimens by spanning the weldment region along the centerline with a 2 in. gage length linear voltage differential-transformer-type extensometer. In a select number of specimens, a 1/16 in. electrical resistance strain gage was employed to sense displacements in the weld metal. An autographic record was made of load versus displacement in these instrumented specimens. However, most of the tensile tests were conducted to determine only the ultimate strength.

Root surface of bead hangs free in backing groove.

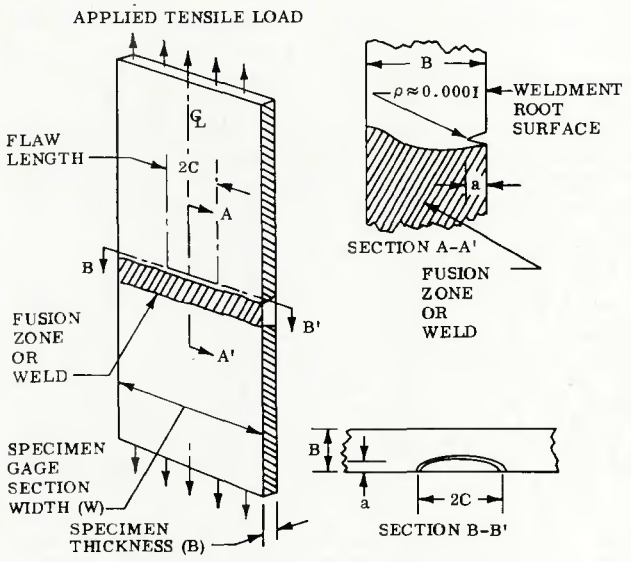

Fig. 1 — Part-through-thickness surface-flawed toughness specimen. The flaw may be a mechanically sharpened slot as illustrated or a fatigue crack

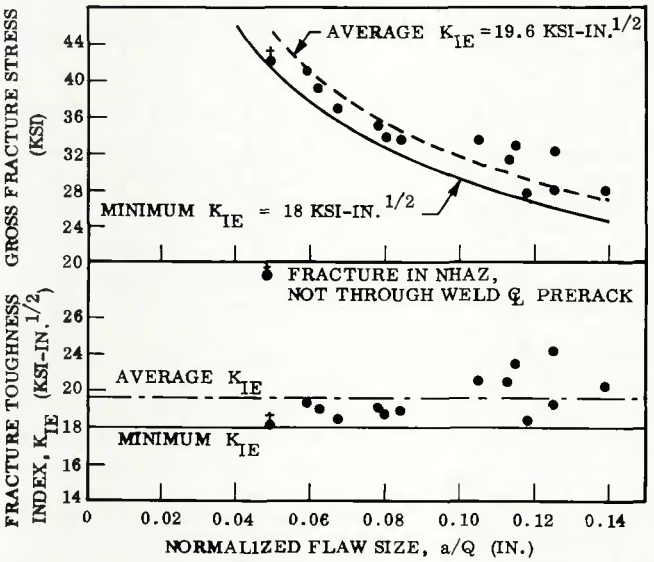

Fig. 2 — Fracture toughness data for 0.33 in. thick 2021 aluminum alloy weldments. The surface flaw is located in the weld centerline on the root side. All tests conducted at room temperature

Fracture Toughness Test Procedure

In the first specimens tested, a clip gage of special design was used to sense crack opening displacement. An autographic record was made of load versus crack opening displacement for each of these specimens. However, no significant variations were noted in these records until the fracture load was attained. Consequently, on subsequent test specimens, only the maximum fracture load was recorded and used to calculate the fracture toughness index, K_{IE}.

Test specimens were monotonically tension loaded to failure in a Universal testing machine at nominal cross head displacement rate of 0.02 in./min. Wedge grips were used to secure the specimen ends. All tests were conducted at room temperature.

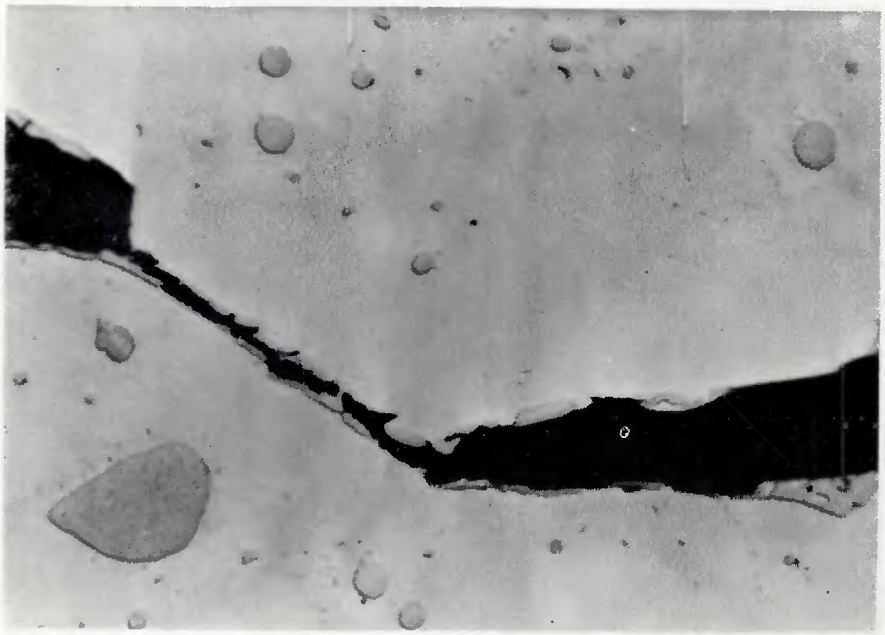

Fig. 3 — Cross-section of welded specimen produced by the primary fabrication condition. Crack propagated preferentially through the intermetallic compound of apparent low toughness that is situated along the grain boundaries in the near heat-affected zone. X3000, reduced 24%

Experimental Results and Discussions

Tensile Tests

Tensile tests were employed to evaluate the mechanical integrity of the weldments in their various conditions of processing. The conditions evaluated include: as-welded (primary weld procedure only); welded and postweld aged; welded, mechanically straightened and postweld aged; and, welded with plus and minus 10 ampere variations in the welding current of the standard weld procedure plus postweld age. In most instances, the ultimate strength was the only information obtained from the tensile tests.

As-welded tensile properties of the weldments are: a 0.2% offset yield strength of 26.4 ksi measured with a 2 in. gage length extensometer, and an ultimate strength of 39.9 ksi. Fracture in these specimens occurred in the weld metal.

The average 0.2% offset yield strength of the weldments joined by the nominal weld procedure and exposed to a postweld aging treatment as well as those weldments that were mechanically straightened prior to aging is 32 ksi measured with a 2 in. gage length extensometer, and 24 ksi measured with a 1/16 in. gage length foil strain gage positioned in the weld. Ultimate strengths of these weldments ranged from 41.0 to 47.2 ksi, with an average value of 44.4 ksi.

All of the specimens that were obtained from weldment panels that received a postweld aging treatment fractured in the near heat-affected zone, approximately 0.005 to 0.015 in. from the fusion line. This region contains an apparently brittle intermetallic compound in the grain boundaries.

Fracture Toughness Tests

The relationship between fracture stress and flaw size in the weld fusion and near heat-affected zones was determined for the primary fabrication conditions over the entire elastic stress range of interest in the fuel storage pressure vessel; i.e., 24 ksi (operating stress) to 30 ksi (proof stress). In addition, the fracture toughness parameter, K_{IE}, was evaluated for the weld centerline in as-welded, and repair welded plus aged conditions; and for the near heat-affected zone in the as-welded, as-welded and overaged, third pass and aged, repair welded and aged, and as-welded with +10 A and −10 A variation in welding current and aged conditions.

Weld Centerline K_{IE}

To evaluate fracture toughness of the weld fusion zone, produced by the primary fabrication condition, precracks were positioned along the centerline of the weld in as-welded and aged specimens. The results are shown in Fig. 2. The surface-flawed fracture toughness parameter, K_{IE}, for this region ranges from 18 to 22 ksi-in.$^{1/2}$ for normalized flaw sizes, a/Q, from 0.049 to 0.139 in. The average K_{IE} value is 19.6 ksi-in.$^{1/2}$ For the range of normalized flaw sizes tested, the scatter in toughness values increases slightly with increasing a/Q.

One of the specimens that exhibited the minimum toughness value did not fail through the precrack located at the weld centerline but in the near heat-affected zone on the forging side of the weldment. Depth of the precrack in this specimen was measured by sectioning the specimen through the precrack, polishing the surface and examing it at a magnification of 100 diameters. The fracture path through the near heat-affected zone of the forging material is intergranular. Metallographic examination revealed that propagation of the crack was through the intermetallic compound situated along the grain boundaries in this region (see Fig. 3). All other specimens failed through the weld centerline precrack.

Near Heat-Affected Zone K_{IE}

Results of the previous tensile tests and the above anomolous weld centerline fracture toughness test strongly suggested that the heat-affected zone immediately adjacent to the weld edge (0.005 to 0.015 in. from the fusion line) was the weldment region of lowest toughness. Consequently, the subsequent toughness evaluation of the heat-affected zone was of specimens precracked in this area. Because of its location, this specific region is referred to as the near heat-affected zone throughout this paper. The toughness parameter of the near heat-affected zone in weldments produced by the primary welding procedures and aging conditions varied from a low of 11 ksi-in.$^{1/2}$ to a high of 20 ksi-in.$^{1/2}$ with an average value of 15 ksi-in.$^{1/2}$. Normalized flaw sizes ranged from 0.032 to 0.141 in.; fracture strength ranged from 18 to 37 ksi. The data are presented in Fig. 4.

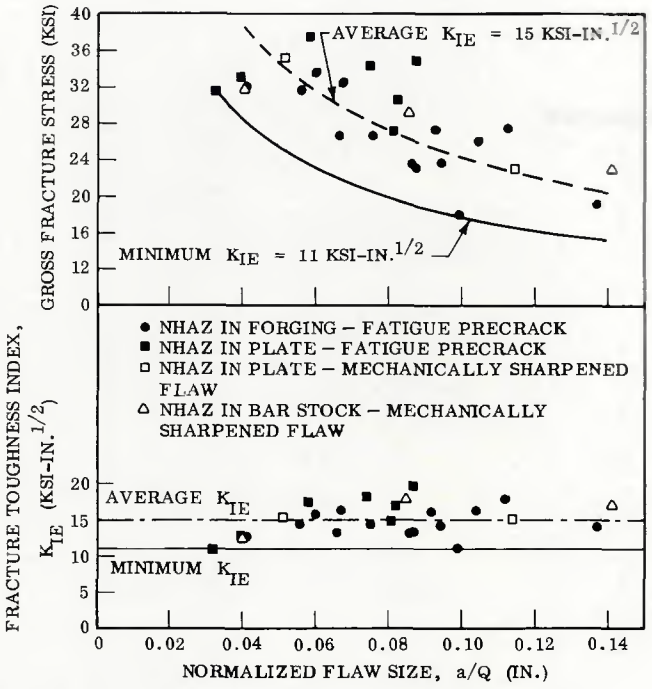

Fig. 4 — Fracture toughness data for 0.33 in. thick 2021 aluminum alloy weldments. The surface flaw is located in the near heat-affected zone (NHAZ) on the root side of the weldment. All tests were conducted at room temperature

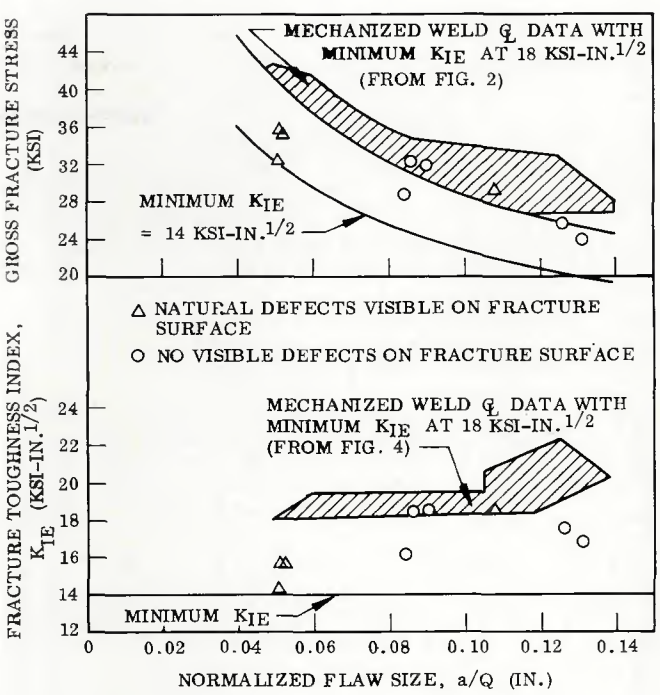

Fig. 5 — Graphical representation of 2021 aluminum weld centerline toughness data for 0.33 in. deep repairs. The surface flaw is on the root side; all tests were conducted at room temperature

The scatter in this data is attributed to two main sources. First, the region of minimum toughness appears to be very narrow — roughly 0.010 in. wide located 0.005 to 0.015 in. from the weld edge — and, therefore, the crack tip may not be positioned precisely in the lowest toughness region in every specimen. The second cause of scatter is the actual variation within each weldment as well as between weldments. The weldments were fabricated over a period of 18 months. Consequently, subtle, unplanned variations from weldment to weldment can be expected.

The profile of the weld varies through the thickness of the specimen. This varying weld metal geometry, coupled with the difficulty in assessing the depth progression of a fatigue crack, makes positioning of the precrack in the desired near heat-affected zone location a formidable task. When the precrack consists only of a mechanically sharpened notch, more control over its proper placement can be exercised. As a result, toughness measurements were performed on a few specimens that contained a mechanical notch, sharpened to a root radius of approximately 0.0001 in., instead of a fatigue precrack. These values are represented by open symbols in Fig. 4. No differences in toughness values attributable to precrack acuity; i.e., mechanically sharpened notch versus fatigue precrack, are discernible.

Although the minimum toughness value in the near heat-affected zone of the bar stock is slightly greater than that of the plate and forging material, all three have approximately the same average value. When the number of samples of each material is considered, the range of toughness values for each are within the same limits.

K_{IE} of Manually Repaired Weldments

A common practice in the fabrication of pressure vessels is to manually repair weld regions that exhibit potentially detrimental defects disclosed by non-destructive inspection. To assess the effect of this rework on the fracture resistance of the weld and the adjacent heat-affected zone, the toughness of these two areas was determined in manually repaired weldments.

In these weldments the repair depth was either 0.25 or 0.33 in., and the length varied from 1 to 2 in. Nine specimens, all with 0.33 in. deep repair welds, were tested to evaluate the toughness in the centerline of the weld; and eight specimens, four with a 0.25 in. deep repair weld and four with a 0.33 in. deep repair weld, were tested to evaluate the toughness in the adjacent near heat-affected zone. All the repairs were made by gouging out a region in a normal mechanized weldment and filling this cavity by gas tungsten-arc welding with 2319 bare filler metal using a multipass stringer bead technique. The data are shown in Fig. 5 for the weld and in Fig. 6 for the near heat-affected zone.

The toughness data from the nine weld centerline specimens range from 14 ksi in.$^{1/2}$ to approximately 18 ksi-in.$^{1/2}$, forming a scatter band contiguous to the lower bound of that for mechanized welds. The limits of the mechanized weld data scatter have been superimposed on Fig. 5 for comparative purposes. In four of the nine specimens, natural weld defects; e.g., porosity, inclusions, and incomplete fusion, were observed on the fracture surfaces. Three of these specimens had the lowest fracture toughness values. As seen in Fig. 5, the manually repaired welds are significantly less tough than the mechanized welds. Evidently, remelted and aged 2021 (mechanized weld) has more fracture resistance than remelted and aged 2319 (manually repaired weld).

Toughness data from the heat-affected zone immediately adjacent to the shallow repaired — 0.25 in. deep — weldments fall within the scatter limits of the near heat-affected zone toughness values for the mechanized weldments produced by the primary fabrication procedures (see Fig. 6). The toughness of the near heat-affected zone in shallow grooved, manually repaired welments and mechanized welds appears to be comparable. A shallow repair — 0.25 in. deep or less — does not significantly alter the fracture characteristics of the mechanized weldment's near heat-affected zone.

On the other hand, the four spec-

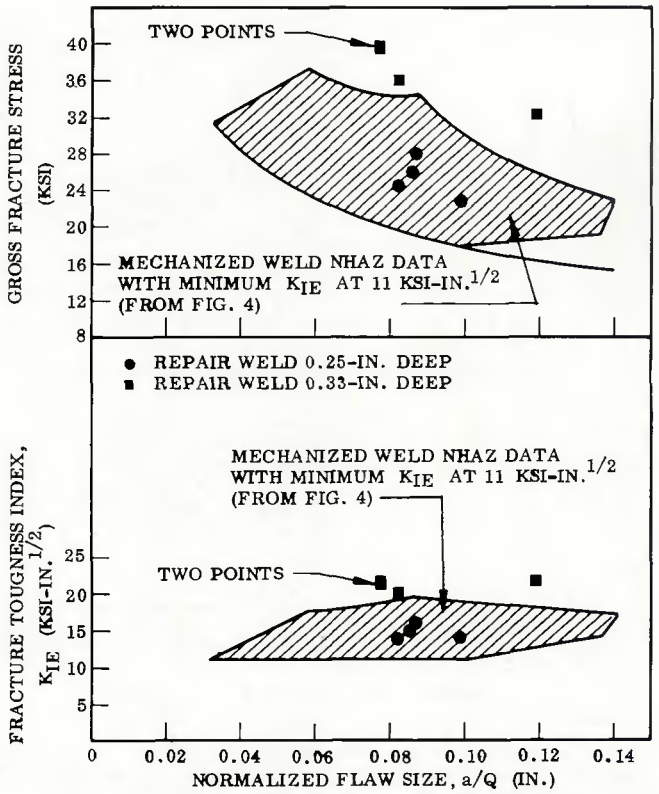

Fig. 6 — Graphical representation of 2021 aluminum near-HAZ toughness data for repaired weldments. The surface is on the root side; all tests were conducted at room temperature

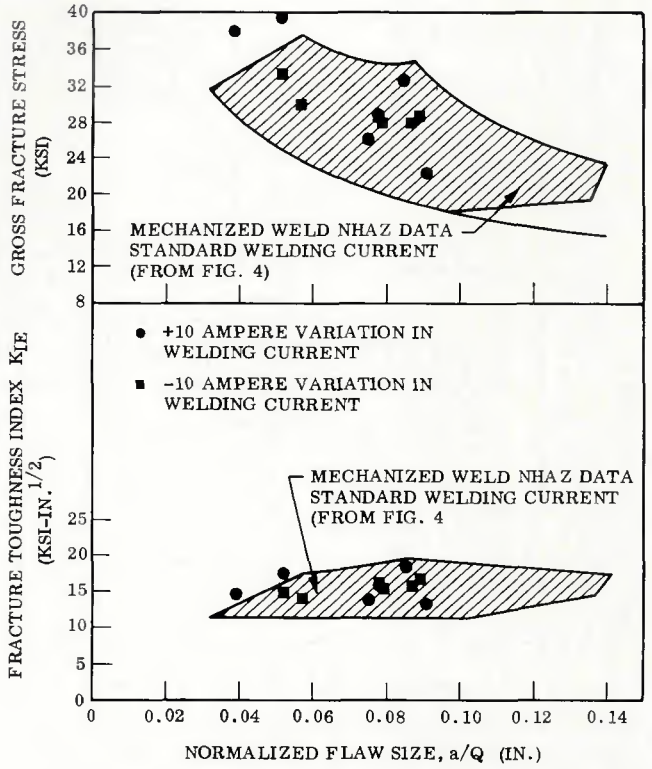

Fig. 7 — Data showing the effect of variation in welding current on near-HAZ toughness in 2021 aluminum alloy suspended bead weldments

imens allotted to evaluate the toughness parameter of the near heat-affected zone bordering deep grooved — 0.33 in. — and manually repaired weldments exhibited significantly higher values than the near heat-affected zone in mechanized weldments.

One of the four specimens tested had the apex of a mechanically sharpened notch positioned in the base metal approximately 0.030 in. from the weld edge (fusion line), a distance of 0.015 to 0.025 in. from the target region. During unstable fracture, the crack propagated laterally from the tip of the notch to the weld edge. The fracture path continued through the specimen along the fusion line, bypassing the near heat-affected zone.

The other three specimens were all fatigue precracked. In one of these precracked specimens, the tip of the starter slot was in the base metal about 0.040 in. from the weld edge, while in the other two, the starter slot tip was situated within the weld approximately 0.005 in. from the weld edge. It was assumed that under the influence of fatigue loading, the precrack would nucleate, grow to and remain in the near heat-affected zone, the region of minimum crack resistance in mechanized welds. Metallographic examination of the specimens, however, showed that fatigue crack extension in all three specimens was to the weld edge and along the fusion line. As in the case of the specimen with the sharpened notch as the flaw, rapid fracture was along the weld edge and not in the near heat-affected zone.

The results from these four tests indicate that the weld edge is apparently less tough than the near heat-affected zone in deep repaired weldments. Additionally, the near heat-affected zone adjacent to a 0.33 in. deep repair weld is significantly tougher than the repaired weld centerline; i.e., greater than 20 ksi-in.$^{1/2}$ versus 14 to 18 ksi-in.$^{1/2}$.

Table 2 — Conditions for Gas Tungsten-Arc Welding 2021 Aluminum Alloy 0.330-In. Thick

	Root Pass	Cover Pass
Welding current	245 A	145A
Welding voltage	10.6 V	15.3 V
Travel speed	10 in./min	10 in./min
Filler metal	None	2319, 1/16 in.
Wire feed	N/A	45 in./min
Gas type and flow:		
Torch side	Helium, 100 cfh	Helium, 100 cfh
Back-up	Argon	N/A
Electrode	1/8 in. diam EWTH2	1/8 in. diam EWTH2
Electrode taper	To 0.065 in.	To 0.065 in.
Nozzle size	5/8 in.	5/8 in.
Joint type	Square butt	Square butt
Preweld cleaning	File, wirebrush, chemically clean, and freon clean	N/A
Weld position:	Vertical [a]	Vertical [a]
Postweld heat treatment	12.5 h at 340 F, A.C.	

(a) Vertical position was used to simulate actual production welding conditions.

Effect of Current Variation on K_{IE}

One of the variations in the primary welding procedure investigated was the permissible + 10 and −10 ampere variation in welding current. Starter slots in the near heat-affected zones of twelve specimens, six fabricated

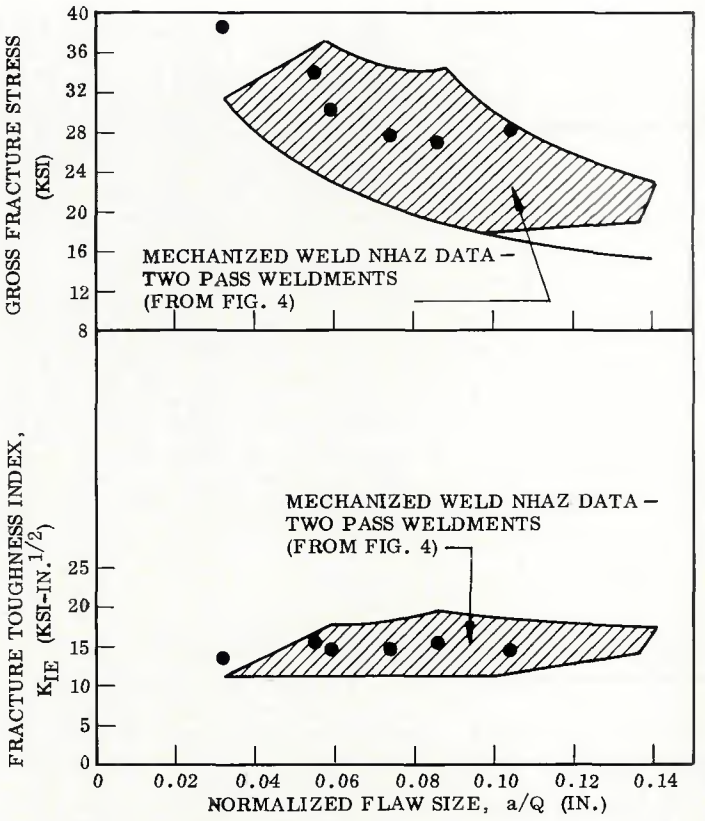

Fig. 8 — Fracture toughness data for 0.33 in. thick 2021 aluminum weldments with a third pass simulating weld start-stop regions. The surface flaw is located in the near-HAZ on the weldments root side. All tests were conducted at room temperature

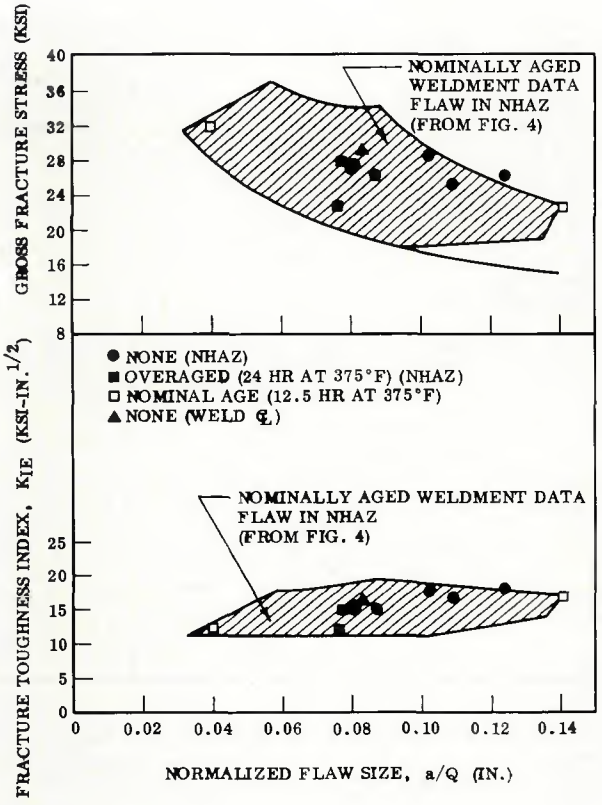

Fig. 9 — Data showing the effect of aging time on near-HAZ toughness in 2021 aluminum alloy suspended bead weldments

with a +10 ampere variation and six with a −10 ampere variation, were sharpened to fatigue crack acuity with cyclic loads and pulled to failure. The results are shown in Fig. 7. Except for a slightly greater spread in the +10 ampere data, no significant difference in fracture toughness is discernible between the two conditions. Both sets of data fall within the scatter limits for specimens fabricated by the primary weld procedure. The data range for specimens joined by the primary weld procedure and shown in Fig. 4 has been superimposed as cross-hatched areas on Fig. 7 for comparative purposes. Although the average ultimate strength varied for weldments fabricated by the three different welding currents, their average fracture toughness index is the same, 15 ksi-in.$^{1/2}$

Effect of Additional Welding Pass on K_{IE}

Often the origin of a pressure vessel failure can be traced to the vicinity of a start-stop region in a closure weld. To simulate such a start-stop region, a weldment was prepared with an additional penetrating pass. Six specimens from the weldments were notched and fatigue precracked in the adjacent near heat-affected zone and tested. The calculated results are shown in Fig. 8. The range of data is much narrower than that from the same region in the standard prepared weldments, represented by the cross-hatched areas in the figure. However, the average toughness value for the two conditions is about the same, 15 ksi-in.$^{1/2}$ Apparently, the performance of an additional welding pass has no marked effect on the toughness of the adjoining near heat-affected zone.

Effect of Postweld Treatment on K_{IE}

In this series of tests, attention was again focused upon the toughness of the near heat-affected zone, the region of lowest toughness in the weldments fabricated and postweld aged as described. Two weldments were fabricated from bar stock panels using the nominal welding technique. Metallographic examination of bar stock and forged samples shows the grain structure to be similar. One weldment was trisected. One section was exposed to the standard postweld aging treatment of 340 F for a period of 12.5 h; another section was overaged at 375 F for a period of 24 h; the third was left as-welded. Two test specimens were then machined from each section. Evaluation of these specimens permits significant differences in toughness to be attributed to the influence of aging alone.

While overaging produces no discernible change in toughness, the minimum toughness in the near heat-affected zone of as-welded specimens appears to be significantly higher than that of aged specimens, 15 ksi-in.$^{1/2}$ compared with 11 ksi-in.$^{1/2}$ (see Fig. 9).

To verify the results of a superior toughness in the as-welded condition, additional tests were conducted on the second weldment. The weldment was left in the as-welded condition and sectioned into five test specimens. Tests performed on four of these specimens confirmed a minimum near heat-affected zone toughness of 15 ksi-in.$^{1/2}$ The fifth specimen was used to evaluate the weld centerline toughness. The result, also shown in Fig. 9, was significantly lower than the minimum for standard aged weldments, 16.4 ksi-in.$^{1/2}$ versus 18 ksi-in.$^{1/2}$

No distinction between the microstructures of as-welded or aged specimens could be detected by metallographic examination. Although the minimum near heat-affected zone toughness is 20% higher in the as-welded condition, there is a sacrifice of 10% in weld metal toughness, and 15 to 20% in mechanical properties.

Table 3 — Summary of Fracture Toughness Results

Weldment region	Condition	Fracture toughness index, K_{IE} Min value, ksi-in.$^{1/2}$	Avg value ksi-in.$^{1/2}$	No. of tests
Weld metal	Welded + aged	18.0	19.6	14
	Deep repair welded + aged	14.0	16.8	9
	As-welded	16.4	16.4	1
Near heat-affected zone	Welded + aged	11.0	15.0	26
	Third pass + aged	14.3	14.6	6
	As-welded	14.8	16.2	6
	Welded + overaged	12.1	13.5	2
	Shallow repair welded + aged	13.6	14.6	4
	Deep repair welded + aged	>19.9	>21.0	4
	Welded with +10A variation in welding current + aged	13.0	15.4	6
	Welded with -10A variation in welding current + aged	13.8	15.2	6

A summary of the surface-flaw fracture results, including minimum value, and number of tests, for each weldment region and condition examined is presented in Table 3.

Conclusions

The conclusions of the experimental study are considered by the authors to be applicable, in general, to 2021 aluminum alloy weldments produced by similar welding procedures and of corresponding thickness. The data may be used for estimation of design allowables but should be experimentally verified before incorporation in a final design.

From the results of the study, several specific conclusions can be made regarding fracture toughness in weldments of the aluminum copper alloy, 2021.

1. Toughness in welds prepared by standard welding procedures and aging treatment (see Table 2) is as follows:
   - Regardless of material form; i.e., plate, forging or bar stock, the near heat-affected zone has the lowest minimum toughness of any weldment region, 11 ksi-in.$^{1/2}$
   - The minimum toughness at the weld centerline is 18 ksi-in.$^{1/2}$, considerably higher than the near heat-affected zone.

2. Variations of ± 10 amperes in welding current or an additional welding pass have no significant effect on the near heat-affected zone toughness.

3. Both the standard (340 F for 12.5 h) and the nonstandard (375 F for 24 h) postweld aging treatments decrease the minimum and average toughness of the near heat-affected zone. However, both postweld aging treatments slightly increase the toughness of the fusion zone.

4. In all cases but one, the near heat-affected zone is less tough than the fusion zone. The exception is the deeply gouged — 0.33 in. — and manually repaired weldment. In this condition, the near heat-affected zone minimum toughness is significantly higher than in a mechanized weldment, > 20 ksi-in.$^{1/2}$ versus 11 ksi-in.$^{1/2}$

References

1. Schultz, R. A., Alcoa Aluminum Alloy 2021, Alcoa Green Letter, Technical Information from Aluminum Company of America, Application Engineering Division, April 1968
2. Carmen, C. M., Iorney, J. W., Katlin, J. M., "Plane Strain Fracture Toughness of 2219-T87 Aluminum Alloy at Room and Cryogenic Temperatures," NASA CR-54297 NASA LeRC, Cleveland, Ohio, August 1966
3. Standard Method of Test for Plane-Strain Fracture Toughness of Metallic Materials, ASTM Designation: E399-72, 1972 Annual Book of ASTM, pp. 955-974
4. Irwin, G.R., "Crack-Extension Force for a Part-Through Crack in a Plate," *J. Appl. Mech.*, Vol. 84, 1962, pp. 651-654
5. Bjeletich, J. G., "The Effect of Flaws on the Fracture Strength of 2021 Aluminum Alloy Sheet Base Metal and Weldment," LMSC Report No. 6-78-68-33, Lockheed Palo Alto Research Laboratory, Aug. 1968